

## Interrelation of transport and optical properties in gold nanoclusters

G. W. Shu, T. Y. Chen, J. L. Shen, C. A. J. Lin, W. H. Chang, W. H. Chan, H. H. Wang, H. I. Yeh, and W. C. Chou

Citation: *Applied Physics Letters* **97**, 123108 (2010); doi: 10.1063/1.3491288

View online: <http://dx.doi.org/10.1063/1.3491288>

View Table of Contents: <http://scitation.aip.org/content/aip/journal/apl/97/12?ver=pdfcov>

Published by the [AIP Publishing](#)

---

### Articles you may be interested in

[Optical properties and refractive index sensitivity of reactive sputtered oxide coatings with embedded Au clusters](#)

*J. Appl. Phys.* **115**, 063512 (2014); 10.1063/1.4861136

[Selective metallization by seeded growth on patterned gold nanoparticle arrays](#)

*J. Appl. Phys.* **113**, 233510 (2013); 10.1063/1.4811229

[Role of ceramic matrix and Au fraction on the morphology and optical properties of cosputtered Au-ceramic thin films](#)

*J. Appl. Phys.* **101**, 113532 (2007); 10.1063/1.2745124

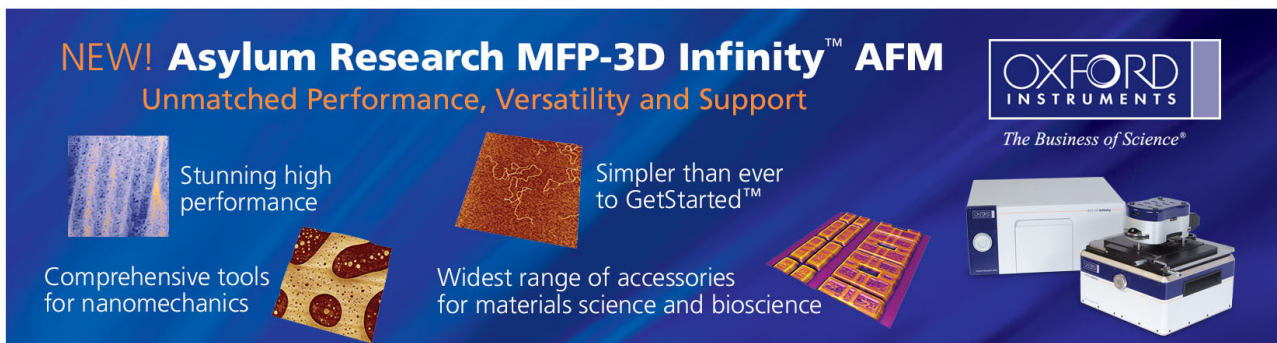
[Electron transfer processes on Ag and Au clusters supported on TiO<sub>2</sub> \(110\) and cluster size effects](#)

*J. Chem. Phys.* **124**, 224710 (2006); 10.1063/1.2205849

[Morphology and transport properties of nanostructural gold on silicon](#)

*J. Appl. Phys.* **95**, 1430 (2004); 10.1063/1.1635989

---

The advertisement features a dark blue background with a grid of images showing various AFM samples and the instrument itself. The text is in white and orange. The Oxford Instruments logo is in the top right corner.

**NEW! Asylum Research MFP-3D Infinity™ AFM**  
Unmatched Performance, Versatility and Support

**OXFORD INSTRUMENTS**  
*The Business of Science®*

Stunning high performance  
Simpler than ever to GetStarted™

Comprehensive tools for nanomechanics  
Widest range of accessories for materials science and bioscience

## Interrelation of transport and optical properties in gold nanoclusters

G. W. Shu,<sup>1</sup> T. Y. Chen,<sup>1</sup> J. L. Shen,<sup>1,a)</sup> C. A. J. Lin,<sup>2</sup> W. H. Chang,<sup>2</sup> W. H. Chan,<sup>3</sup> H. H. Wang,<sup>4</sup> H. I. Yeh,<sup>4</sup> and W. C. Chou<sup>5</sup>

<sup>1</sup>Department of Physics, Chung Yuan Christian University, Chung-Li 32023, Taiwan

<sup>2</sup>Department of Biomedical Engineering, Chung Yuan Christian University, Chung-Li 32023, Taiwan

<sup>3</sup>Department of Bioscience Technology, Chung Yuan Christian University, Chung-Li 32023, Taiwan

<sup>4</sup>Department of Internal Medicine and Medical Research, Mackay Memorial Hospital, Mackay Medical College, Taipei 25160, Taiwan

<sup>5</sup>Department of Electrophysics, National Chiao-Tung University, Hsin-Chu 30010, Taiwan

(Received 17 June 2010; accepted 30 August 2010; published online 23 September 2010)

Temperature dependence of the electrical conductivity and photoluminescence (PL) in Au nanoclusters (NCs) is investigated. The correlation of the conductivity and PL in Au NCs at different temperatures is evident: (i) for  $T < 50$  K, both the conductivity and PL intensity decrease with temperature, which suggests thermal structural fluctuations; (ii) for  $50 \text{ K} < T < 90$  K, conductivity and PL are explained by variable range hopping; (iii) for  $90 \text{ K} < T < 170$  K, simple thermal activated hopping dominates in conductivity, with a rate-equation model proposed to analyze the carrier transfer in PL. © 2010 American Institute of Physics. [doi:10.1063/1.3491288]

Au nanoclusters (NCs) containing  $< 200$  down to a few tens of atoms have attracted significant interest due to their peculiar optical and electronic properties.<sup>1,2</sup> Au NCs can be highly luminescent from visible to near-infrared range. The luminescence in Au NCs is expected to be useful in biological labeling, light emitting diodes, and optoelectronic logic gates.<sup>3-6</sup> Some of the possible applications for NCs involve the recombination and transport of charge carriers through NCs. Therefore, the basic optical and transport properties of the Au NCs must be understood prior to application in devices. Recently, photoluminescence (PL) properties in Au NCs have been reported.<sup>3-6</sup> The PL from the Au NCs could be viewed as a radiative recombination from the highest occupied molecular orbital to the lowest unoccupied molecular orbital transition, and from Fermi level electrons to occupied d-band holes.<sup>5,6</sup> Moreover, the transport properties in Au NCs have been studied in recent years.<sup>7-9</sup> The Mott type insulator-to-metal transition of aggregates of Au NCs has been observed when the average distance of NCs decreases to below 1 nm.<sup>7</sup> Additionally, simultaneous hole- and electron-injections into discrete states and the electron-transfer dynamics based on the voltammetric charge transport measurements are demonstrated.<sup>8,9</sup>

For the photoexcitation of the Au NCs, the carriers generated at excited energy levels may relax into a lower energy level or be recaptured by neighboring NCs, similar to the behavior of quantum dots.<sup>10</sup> In particular, when the temperature ( $T$ ) is increased, the thermally activated carrier transfer or thermally carrier escape among NCs will redistribute the carriers within the energy states.<sup>10</sup> These carrier transfer and/or recombination processes can affect the carrier distribution in the energy states, influencing device performance. While a number of investigations have been performed into the Au NCs, little attention has been given to the relationship between the optical and transport properties, or the carrier charge transfer in Au NCs. This study investigates the electrical conductivity and PL in Au NCs. The  $T$  dependence of

PL intensity is found to be closely associated with that of electrical conductivity.

The Au NCs with dodecanethiol (DDT) were prepared based on a modified Peng reaction.<sup>11</sup> The details of the growth method are described in literature.<sup>12</sup> Briefly, the gold precursor solution was prepared by dissolving  $\text{AuCl}_3$  in a didodecyldimethylammonium bromide solution. Decanoic acid was then combined with tetrabutylammonium borohydride in toluene, followed by the gold precursor solution. The synthesized Au colloids were further fragmented by adding the precursor solution, leading to formation of smaller Au NCs. The Au NCs with DDT were obtained by adding DDT in toluene, except the precursor solution. The particle size of Au NCs with DDT was estimated at  $1.9 \pm 0.2$  nm from transmission electron microscopy, as displayed in Fig. 1(a). The solid-state Au NCs were formed on lithographically patterned silicon substrates by the drop-casting method upon evaporation of the solvent.<sup>13</sup> The electrical conductivity was measured in a simple two electrode configuration,<sup>14</sup> where a bias voltage ( $V$ ) was applied by an electrometer

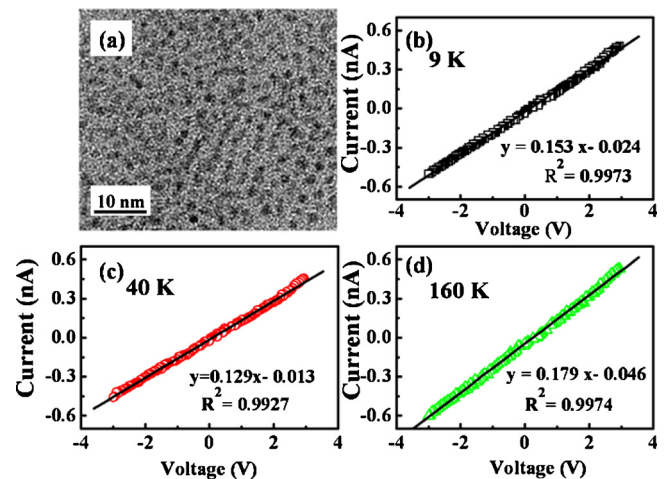


FIG. 1. (Color online) (a) The high-resolution transmission electron microscopy image for the Au NCs. The measured I-V curves from the Au NCs with different  $T$ : (b) 9 K, (c) 40 K, and (d) 160 K. The correlation equations and values of squares of correlation coefficient  $R^2$  are included.

<sup>a)</sup> Author to whom correspondence should be addressed. Electronic mail: jlshen@cycu.edu.tw.

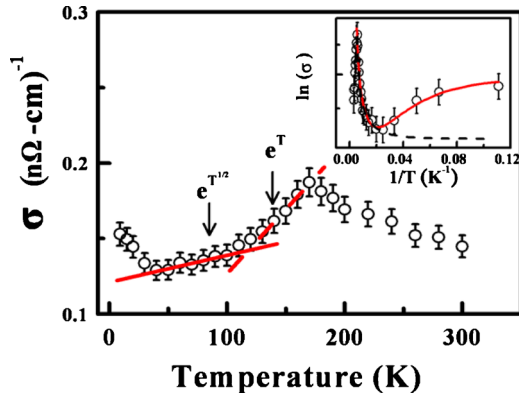


FIG. 2. (Color online) Variation in conductivity with  $T$  for the Au NCs. The dashed (solid) line is the simulated curve with the simple thermally activated process (the variable range hopping process). The inset displays a plot of conductivity vs the inverse  $T$ . The dashed (solid) line in the inset is a fitted result without (with) considering the thermal structural fluctuations.

across two electrodes attached to a sample, and the resulting current ( $I$ ) was measured. Changes as small as  $10^{-9}$  S/cm $^{-1}$  can be measured using this setup.  $I$ - $V$  characteristics curves were measured over a range from 10 to 300 K, using a cold finger of a closed-cycle helium cryostat. For the PL measurements, a diode laser with a wavelength of 470 nm and an average power density of 1.2 W/cm $^2$  was used as an excitation source. The PL was collected in backscattered geometry by a spectrometer, and detected using a cooled GaAs photomultiplier tube. Spectra were collected at a resolution of 1 cm $^{-1}$ .

Figure 1 displays the current-voltage characteristics of Au NCs for some  $T$ . On the basis of least square fittings, the correlation equations between current and voltage, as well as values of squares of correlation coefficient  $R^2$ , are shown in Figs. 1(b)–1(d). As seen, there is a satisfactory linear correlation between the current and voltage ( $R^2$  within 0.9927–0.9974), indicating the Ohmic response. The room-temperature conductivity of the Au NCs is  $\sim 2 \times 10^{-7}$  S/cm $^{-1}$ , in good agreement with that of similar C $_{12}$ -capped Au NCs.<sup>15</sup> Figure 2 shows the variation of conductivity with  $T$ . For  $T > 170$  K, conductivity increases with the decreasing  $T$ . This trend indicates a positive  $T$  coefficient of resistance, consistent with metallic behavior. For  $T < 170$  K, conductivity shows a cross-over to a different regime, where the  $T$  coefficient of resistance is negative. This metal-nonmetal transition has been recently investigated in metal nanoparticles.<sup>14,16</sup> For  $170 \text{ K} > T > 90 \text{ K}$ , the conductivity in the Au NCs decreases exponentially with  $T$  as  $\exp(-E_a/kT)$  ( $E_a$  is the thermal activation energy), indicated by the dashed line in Fig. 2, and revealing a simple thermally activated hopping.<sup>14</sup> In this hopping process, the conduction is shown by the decreased population of thermally activated carriers from localized to delocalized states by lowering  $T$ .

As  $T$  is decreased from 90 to 50 K, conductivity decreases with  $\exp(T^{1/2})$ , displayed by the solid line in Fig. 2. The  $\exp(T^{1/2})$  law has been previously found in the transport experiments in metal nanoparticles.<sup>14,16,17</sup> This behavior can be explained by the variable range hopping (VRH), where a charge carrier would jump a distance to maximize the hopping rate between the occupied and unoccupied states.<sup>14</sup> For  $50 \text{ K} < T < 170 \text{ K}$ , the conductivity is a manifestation of the switching mechanism from an activated hopping at high  $T$  to a VRH behavior at low  $T$ . To describe the coexistence regime

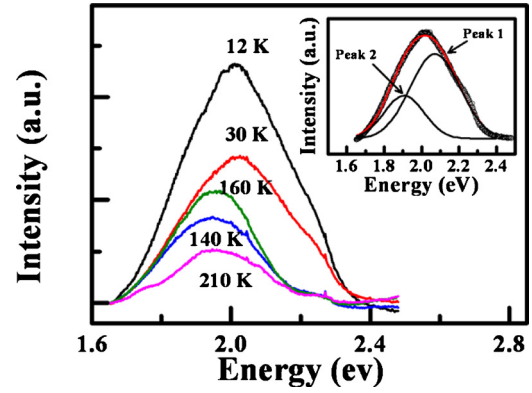


FIG. 3. (Color online) PL spectra of Au NCs at different  $T$ . The inset shows the PL spectrum of the Au NCs at 12 K (open circles) with PL resolved by a two-Gaussian fitting.

of the VRH and thermally activated hopping, a combined form of the above two mechanisms are used, as follows:<sup>17</sup>

$$\sigma_1 = A_1 \times \exp\left[-\left(\frac{E_a}{kT}\right)\right] + A_2 \times \exp\left[-\left(\frac{E_{\text{VRH}}}{kT}\right)^{1/2}\right], \quad (1)$$

where  $E_{\text{VRH}}$  is the activation energy for VRH. The calculation according to Eq. (1) is plotted as the dashed line in the inset of Fig. 2. The fit is not appropriate to describe the conductivity for  $T < 50$  K. To explain conductivity below 50 K, the conductivity due to VRH can be described by  $E_{\text{VRH}} = \Delta a \alpha$ , where  $\Delta$  characterizes the strength of static disorder,  $a$  as the distance between the nearest neighbor, and  $\alpha$  is the inverse localization length.<sup>18</sup> We assume  $\alpha$  is affected by the thermal structural fluctuations and written as<sup>18</sup>

$$\alpha = \alpha_0 + \alpha_1 \tanh\left(\frac{T_d}{T}\right), \quad (2)$$

where  $\alpha_0$  is static disorder,  $\alpha_1$  is thermal structural fluctuations, and  $T_d$  is a parameter associated with the twist angle fluctuations. If  $E_{\text{VRH}}$  in Eq. (1) is replaced by  $\Delta a \alpha$ , then the solid line in the inset of Fig. 2 displays the calculation with thermal structural fluctuations. A good agreement with experiments suggests that the conductivity for  $T < 50$  K is mostly influenced by the thermal structural fluctuations.

Figure 3 displays the PL spectra of Au NCs with different  $T$ . The dashed lines in the inset of Fig. 3 display the two Gaussian components of the 12-K PL, assigning the high-energy and low-energy peak as the peak H and peak L, respectively. The open circles and squares in Fig. 4 show the PL intensities versus  $T$  for peaks H and L. The PL intensity for peak H is decreased, however, it reduces more rapidly for  $T < 50$  K and  $170 \text{ K} > T > 90 \text{ K}$ . On the other hand, the PL intensity for peak L decreases with  $T$  for  $T < 90 \text{ K}$ , and then increases with  $T$  from 90 to 170 K. As  $T > 170 \text{ K}$ , the PL intensity decreases.

Comparing Fig. 4 with Fig. 2, it is notable that these two figures have same crossover  $T$ , namely, 50, 90, and 170 K. We, therefore, suggest that the PL intensities can be related to conductivity as follow: (i) For  $T < 50 \text{ K}$ , the carrier scattering increases due to the VRH with thermal structural fluctuations, giving the carriers more opportunity to be trapped. This behavior reduces both the conductivity and PL intensity. (ii) For  $50 \text{ K} < T < 90 \text{ K}$ , the VRH dominates the conductivity. The PL intensity continues decreasing because the thermally excited carriers can acquire energy and hop to an



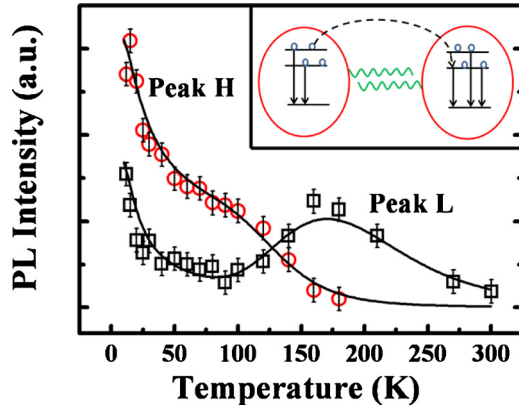


FIG. 4. (Color online) PL intensities in Au NCs vs T for the peak H (open circles) and peak L (open squares). The solid lines show the fitted results according to Eqs. (5)–(7). The inset displays a schematic describing the charge carrier transfer in the Au NCs.

other site. (iii) For  $90 \text{ K} < T < 170 \text{ K}$ , a part of the carrier in the high-energy level may be scattered into the low-energy level through simple thermally activated hopping. Thus, the carriers in the low-energy level increase due to this hopping. A rate equation model is used to analyze the PL intensities. In a first approximation two neighboring Au NCs, separated by the distance of a DDT molecule (as shown in the inset of Fig. 4) are considered. According to this model, the rates of carrier density in NCs are given by the following:

$$\frac{dn_H(T)}{dt} = C_H - n_H(T)R_H(T) - n_H(T)N_{H1}(T) - n_H(T)N_{H2}(T) - n_H(T)N_{H3}(T), \quad (3)$$

$$\frac{dn_L(T)}{dt} = C_L - n_L(T)R_L(T) - n_L(T)N_{L1}(T) - n_L(T)N_{L2}(T) - n_L(T)N_{L3}(T) + n_H(T)N_{H3}(T), \quad (4)$$

where  $n_H(T)$  [ $n_L(T)$ ] is the carrier density in the high-(low-) energy level;  $C_H$  ( $C_L$ ) is the number of carriers per second captured in the high-(low-) energy level at 0 K;  $R_H(T)$  [ $R_L(T)$ ] is the radiative recombination rate for  $n_H(T)$  [ $n_L(T)$ ]; and  $N_{Hi}(T)$  [ $N_{Li}(T)$ ] (where  $i=1, 2$ , and  $3$ ) is the nonradiative recombination rate for  $n_H(T)$  [ $n_L(T)$ ]. Given the thermal distribution, a part of the carriers is thermally escaped according to the following:

$$N_{ji}(T) = a_{ji} \exp(-E_{ji}/k_B T) \text{ (where } j = H \text{ and } L; i = 1, 2, \text{ and } 3), \quad (5)$$

where  $a_{ji}$  is a constant and  $E_{ji}$  is the activation energy.

By considering luminescence intensity is proportional to the carrier density and quantum yield, the PL intensity for peak H(L) can be calculated, as follows:

$$I_H = \frac{C_H}{R_H} \left[ \frac{R_H}{R_H + N_{H1}(T) + N_{H2}(T) + N_{H3}(T)} \right]^2, \quad (6)$$

$$I_L = \frac{C_L}{[R_L + N_{L1}(T) + N_{L2}(T) + N_{L3}(T)]^2} \left[ 1 + \frac{C_H}{C_L} \times \frac{N_{H3}(T)}{R_H + N_{H1}(T) + N_{H2}(T) + N_{H3}(T)} \right]. \quad (7)$$

Equations (5)–(7) allow us to fit the PL intensity. The

TABLE I. The activation energies  $E_{ji}$  and constants  $a_{ji}$  used in the fits according to Eq. (5).

$E_{H1}$ (meV)	$E_{H2}$ (meV)	$E_{H3}$ (meV)	$E_{L1}$ (meV)	$E_{L2}$ (meV)	$E_{L3}$ (meV)
3.5	20	69	3.5	20	101
$a_{H1}$	$a_{H2}$	$a_{H3}$	$a_{L1}$	$a_{L2}$	$a_{L3}$
0.9	0.5	222	2	2.5	333

parameters used in the fit are listed in Table I. The solid lines in Fig. 4 give the fits, in reasonable agreement with the experiment. Thus, the T dependence of PL intensity can be described in the framework of the rate equation model, taking into account of the carrier transfer between the emitting states.

In summary, the correlation of the conductivity and PL of the Au NCs is evident at different T: (i) For  $T < 50 \text{ K}$ , the scattering of carriers increases with T due to the thermal structural fluctuations, leading to an increase in trapped carriers and reducing both the conductivity and PL intensity. (ii) For  $50 \text{ K} < T < 90 \text{ K}$ , the VRH mechanism reveals domination of the conductivity. The PL intensity continues decreasing as the carriers hop to another site. (iii) For  $90 \text{ K} < T < 170 \text{ K}$ , the conductivity is described by simple thermally activated hopping. A rate-equation model is proposed for the carrier charge transfer between the emitting states.

This project was supported by the National Science Council under the Grant No. NSC 98-2627-B-033-002.

<sup>1</sup>G. Hodes, *Adv. Mater.* **19**, 639 (2007).

<sup>2</sup>H. Häkkinen, R. N. Barnett, and U. Landman, *Phys. Rev. Lett.* **82**, 3264 (1999).

<sup>3</sup>T. A. Lee, J. I. Gonzalez, J. Zheng, and R. M. Dickson, *Acc. Chem. Res.* **38**, 534 (2005).

<sup>4</sup>S. Link, A. Beeby, S. FitzGerald, M. A. El-Sayed, T. G. Schaaff, and R. L. Whetten, *J. Phys. Chem. B* **106**, 3410 (2002).

<sup>5</sup>Y. Bao, C. Zhong, D. M. Vu, J. P. Temirov, R. B. Dyer, and J. S. Martinez, *J. Phys. Chem. C* **111**, 12194 (2007).

<sup>6</sup>D. Lee, R. L. Donkers, G. Wang, A. S. Harper, and R. W. Murray, *J. Am. Chem. Soc.* **126**, 6193 (2004).

<sup>7</sup>S. H. Kim, S. Hwang, Y. S. Shon, D. F. Ogletree, and M. Salmeron, *Phys. Rev. B* **73**, 155406 (2006).

<sup>8</sup>J. I. Gonzalez, T. Vosch, and R. M. Dickson, *Phys. Rev. B* **74**, 235404 (2006).

<sup>9</sup>D. Lee, R. L. Donkers, J. M. DeSimone, and R. W. Murray, *J. Am. Chem. Soc.* **125**, 1182 (2003).

<sup>10</sup>C. Lobo, R. Leon, S. Marcinkevicius, W. Yang, P. C. Sercel, X. Z. Liao, J. Zou, and D. J. H. Cockayne, *Phys. Rev. B* **60**, 16647 (1999).

<sup>11</sup>N. R. Jana and X. G. Peng, *J. Am. Chem. Soc.* **125**, 14280 (2003).

<sup>12</sup>M. D. Yang, Y. K. Liu, J. L. Shen, C. H. Wu, C. A. Lin, W. H. Chang, H. H. Wang, H. I. Yeh, W. H. Chan, and W. J. Parak, *Opt. Express* **16**, 15754 (2008).

<sup>13</sup>R. P. Andres, J. D. Bielefeld, J. I. Henderson, D. B. Janes, V. R. Kola-gunta, C. P. Kubiak, W. J. Mahoney, and R. G. Osifchin, *Science* **273**, 1690 (1996).

<sup>14</sup>A. Zabet-Khosousi and A. A. Dhirani, *Chem. Rev.* **108**, 4072 (2008).

<sup>15</sup>W. P. Wuelfing, S. J. Green, J. J. Pietron, D. E. Cliffler, and R. W. Murray, *J. Am. Chem. Soc.* **122**, 11465 (2000).

<sup>16</sup>A. Zabet-Khosousi, P. E. Trudeau, Y. Saganuma, and A. A. Dhirani, *Phys. Rev. Lett.* **96**, 156403 (2006).

<sup>17</sup>F. Remacle, K. C. Beverly, J. R. Heath, and R. D. Levine, *J. Phys. Chem. B* **106**, 4116 (2002).

<sup>18</sup>Z. G. Yu and X. Song, *Phys. Rev. Lett.* **86**, 6018 (2001).